01 Aug 2019

Remote Sensing of Explosives-Induced Stress in Plants: Hyperspectral Imaging Analysis for Remote Detection of Unexploded Threats

Paul V. Manley

Vasit Sagan

Felix B. Fritschi

Joel Gerard Burken
Missouri University of Science and Technology, burken@mst.edu

Recommended Citation

P. V. Manley et al., "Remote Sensing of Explosives-Induced Stress in Plants: Hyperspectral Imaging Analysis for Remote Detection of Unexploded Threats," *Remote Sensing*, vol. 11, no. 15, MDPI AG, Aug 2019.
The definitive version is available at https://doi.org/10.3390/rs11151827

remote sensing

MDPI

Article

Remote Sensing of Explosives-Induced Stress in Plants: Hyperspectral Imaging Analysis for Remote Detection of Unexploded Threats

Paul V. Manley [1,*], Vasit Sagan [2], Felix B. Fritschi [3] and Joel G. Burken [1]

[1] Department of Civil, Architectural, and Environmental Engineering, Missouri University of Science and Technology, Rolla, MO 65409, USA
[2] Department of Earth and Atmospheric Sciences, Saint Louis University, St. Louis, MO 63108, USA
[3] Division of Plant Sciences, University of Missouri, Columbia, MO 65211, USA
* Correspondence: pvm88b@mst.edu

Received: 10 June 2019; Accepted: 3 August 2019; Published: 5 August 2019

Abstract: Explosives contaminate millions of hectares from various sources (partial detonations, improper storage, and release from production and transport) that can be life-threatening, e.g., landmines and unexploded ordnance. Exposure to and uptake of explosives can also negatively impact plant health, and these factors can be can be remotely sensed. Stress induction was remotely sensed via a whole-plant hyperspectral imaging system as two genotypes of *Zea mays*, a drought-susceptible hybrid and a drought-tolerant hybrid, and a forage *Sorghum bicolor* were grown in a greenhouse with one control group, one group maintained at 60% soil field capacity, and a third exposed to 250 mg kg^{-1} Royal Demolition Explosive (RDX). Green-Red Vegetation Index (GRVI), Photochemical Reflectance Index (PRI), Modified Red Edge Simple Ratio (MRESR), and Vogelmann Red Edge Index 1 (VREI1) were reduced due to presence of explosives. Principal component analyses of reflectance indices separated plants exposed to RDX from control and drought plants. Reflectance of *Z. mays* hybrids was increased from RDX in green and red wavelengths, while reduced in near-infrared wavelengths. Drought *Z. mays* reflectance was lower in green, red, and NIR regions. *S. bicolor* grown with RDX reflected more in green, red, and NIR wavelengths. The spectra and their derivatives will be beneficial for developing explosive-specific indices to accurately identify plants in contaminated soil. This study is the first to demonstrate potential to delineate subsurface explosives over large areas using remote sensing of vegetation with aerial-based hyperspectral systems.

Keywords: Hyperspectral imaging; plant stress; phytoforensics; explosives; RDX; drought

1. Introduction

Environmental contamination by explosives and energetics has resulted from widespread production, testing and partial detonations, unexploded ordnance (UXO), and improper disposal. Unique to these constituents, threats exist for acute and chronic health concerns [1], and even physical threats by UXO. Landmines are of specific concern as over 110 million have been laid in more than 70 countries since the 1970s [2]. An estimated 15,000 to 20,000 people are injured or killed each year from remnant landmines, with children accounting for one in five of those deaths [3]. Current landmine detection methods often consider vegetation a hindrance, though plants can aid in more rapid discovery if used as phytosensors in the delineation and remediation effort.

While landmines are dangerous, explosives contamination in soil is of serious concern for a variety of reasons. It is estimated that in the US alone 10 million hectares need remediation [4]. Royal demolition explosive (RDX; hexahydro-1,3,5-trinitro-1,3,5-triazine) is commonly found with trinitrotoluene (TNT)

in soil and is highly mobile unlike TNT and has entered groundwater sources of some communities around military bases [5]. With almost 2000 sites at closed military bases contaminated with UXO, explosives contamination at military testing sites also complicate base conversions after closure [6,7]. Over the course of years of being in soil, ordnance casings containing RDX degrade from contact with water in the form of rain and soil moisture [8]. The sheer volume and diversity of fugitive compounds in the subsurface drives the need for a novel technique that accurately locates contaminants and will allow for safe and rapid remediation.

Plants can be used as sentinels to discover what lies in soil beneath the surface. Roots spread out in the subsurface and acquire water, nutrients, and many chemicals present in subsurface soil and groundwater, thereby acting as an in-situ sampling tool. Chemical testing of plant tissues has shown that plants can act as chemical samplers [9] and that uptake is predicted by physio-chemical properties [10]. Compounds that can cross root membranes may cause stress by altering physiological and morphological characteristics, e.g., chlorophyll reductions, decreased stomatal conductance, increased fluorescence, and reduced biomass. Explosives enter plants by crossing root membranes via bulk water transport and are either stored in roots or translocated to leaves where they accumulate [11–13]. RDX is known to cause plant stress at relatively low concentrations [14]. RDX is a nitroamine that readily moves into plants and is translocated into aerial portions of plants where it negatively affects leaf function and health.

Plant stress can be caused by a variety of factors such as nutrient deficiencies or pests, and often manifests by way of reductions in pigment concentrations, decreased photosynthesis, necrosis, and changes in plant morphology and physiology are remotely detectable with hyperspectral imagery (HSI) [15]. Plant stress responses caused by environmental pollutants such as explosives can be remotely detected via hyperspectral sensors [14,16] leading to the possibility of scaling up detection to the field level. Importantly, to be effective in remotely detecting a specific contaminant, it is necessary to compare numerous sources of stress and differentiate between them to limit potential false positives or negatives. As plant responses can be species- and explosive-specific, discriminating between both natural, i.e., drought or nutrient deficiency, and anthropogenic stressors is crucial for the accurate remote detection of explosives. Research is extremely limited on comparing drought conditions to plant stress caused by explosives [16]. Some studies have explored uptake of explosives by agronomic species [13,17] and how the reflectance of shrubs is affected by explosives [14,16,18], but none have done both. The research presented here was conducted in conjunction with a field-scale drought experiment that utilized the same genotypes assessed with the same aerial-based HSI methods.

Hyperspectral imagery has been utilized for decades on vegetation for early stress detection to mitigate potential agricultural crop losses. Other instances include using HSI of vegetation for the detection of heavy metal contamination and salt stress [19,20]. Minimal research has been directed at using plants to detect explosives in soil. Previous energetics detection work involved using handheld spectroradiometers to obtain reflectance of leaves and calculating reflectance indices [14,18]. Reflectance Index values were compared to plant functional traits, and it was found that stomatal conductance and photosynthesis were negatively affected by concentrations as low as 100 mg kg^{-1} RDX in soil, while pigment concentrations were decreased beginning at 500 mg kg^{-1} RDX for the coastal pioneer species, *Baccharis halimifolia* [14].

The objective of this contribution was to begin developing effective methods of detecting plant stress from explosives by comparing distinct hyperspectral reflectance signatures of drought and RDX-exposed plants at a species-specific level for canopy-wide application. Existing reflectance indices were examined in this study to determine their efficacy in differentiating between natural and anthropogenic stressors remotely. Measuring reflectance at specific wavelengths sensitive to the presence of explosives is crucial and a prerequisite to the implementation of this research in real-world scenarios. While this paper only discusses imagery, the findings within are promising. It remains imperative to continue similar research to hasten the detection rates of remnant landmines and other sources of explosives contamination.

2. Materials and Methods

2.1. Plants

Two hybrids of *Zea mays* L. (maize) and one of *Sorghum bicolor* (L.) Moench (sorghum) were grown in a greenhouse at Missouri University of Science and Technology, Rolla, MO (37.955376 N, 91.771681 W). One maize hybrid (Pioneer® P1690AM, DuPont®, Wilmington, DE; abbreviated here as 'AM') was considered less drought tolerant than the other (Pioneer® P0363AMX, DuPont®, Wilmington, DE; abbreviated here as 'AMX'). The sorghum used was forage sorghum (Blade® EJ 7282, Ceres, Inc., Boston, MA), referred to here as 'S'. Plants in the drought and control groups were germinated in 38 L pots (Hummert™ International Treepots™, Earth City, MO) filled with 14 kg of soil (Mexico silt loam soil; fine, smectitic, mesic, Vertic Epiaqualf) per pot that was collected from University of Missouri's Bradford Research Center near Columbia, MO (38.894167 N, 92.201389 W). Plants used for the RDX treatment were germinated in small pots and transplanted to contaminated soils to mitigate effects of explosives on germination. Each group consisted of eight plants for a total of 72 plants. However, two plants died during the experiment: one control sorghum plant and one RDX-exposed AM maize plant. Plants were grown in a greenhouse under natural sun light which was supplemented by LumiGrow Pro325™ (LumiGrow, Inc) LED lights to extend the photoperiod to 14 h.

To prepare the RDX-contaminated soil, RDX (1,3,5-trinitro-1,3,5-triazinane) was dissolved in acetone at a concentration of 10 g L^{-1}. This stock solution was diluted to dose soils at a concentration of 250 mg kg^{-1}. Soil for control and drought plants were also dosed with acetone to control for any potential acetone effects. Drought treatment plants were held at 60% field capacity (FC) and control plants were held at 90% FC by weighing each pot daily and replacing the lost water to return the soil to 60% and 90% FC, respectively. Field capacity was measured by taking a known mass of soil and completely saturating it with water, allowing water to drain for two days and weighing soil after draining. The soil sample was left to dry completely in the greenhouse and weighed again. The gravity drained soil was taken as 100% FC and the air-dried soil sample considered to be at 0% FC and were used to calculate the appropriate FC.

2.2. Hyperspectral Imaging

Hyperspectral images were collected at the end of a four-week period after start of experiment with a Headwall Nano-Hyperspec (VNIR) imager (Headwall Photonics, Inc., Bolton, MA, USA). This sensor collects spectral information for 274 bands from 400–1000 nm at 2 nm intervals with a Full-Width Half-Maximum (FWHM) of around 5 nm. The last two bands were removed from all images during pre-processing to eliminate noise. A halogen lamp was used as a full-spectrum artificial light source to control lighting and to mitigate any atmospheric corrections required from using the sun for illumination. Using an artificial light source also allows for consistent imaging despite weather conditions. A 10" square Labsphere Spectralon®white reflectance standard was used only for light calibration; dark calibration was done using the lens cap. The headwall sensor was mounted in a nadir position to a custom-made, 3 m-tall gantry system (Figure 1) that used a lead screw to move the sensor at a rate of 0.635 m min^{-1} at 1.2 m above canopy to image each plant individually. The gantry system allows for line-scanning of whole plants and mimics the line-scanning methods also applied at a field-scale with an unmanned aerial vehicle. Plant heights did not vary appreciably in the greenhouse study.

Eighteen relevant, established reflectance indices demonstrated to correlate with plant functional traits (Table 1) were calculated from plant HSI using ENVI (Environment for Visualizing Images, Harris Geospatial Solutions, Inc., Denver, CO, USA) from the list of available reflectance indices integrated into the software. Custom interactive data language (IDL) codes were written for ENVI to handle batch processes. The first code masked the background of each image, computed reflectance indices for Index averages, and output those values to a text file (Figure 2). Another custom IDL code used the masked images to extract average spectral values for each plant. Every pixel of each image, after

masking, was used for analyses. Reflectance indices and spectra were calculated for each pixel and then averaged per plant. Individual plant reflectance spectra were then averaged together by group and plotted in Excel (Microsoft Corporation, Redmond, WA, USA). First derivatives, or the change in slope, were calculated from reflectance spectra in Excel. Results are plotted by plant type.

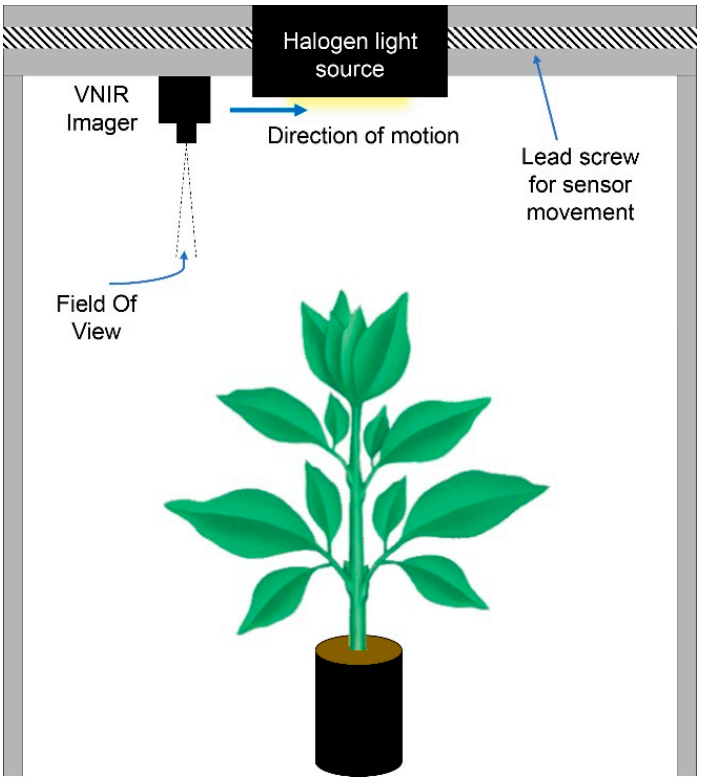

Figure 1. Schematic of the 3-m tall custom-built gantry system for sensor movement. The sensor is moved along a defined track by a lead screw. The halogen light source provides full spectrum artificial illumination for the object.

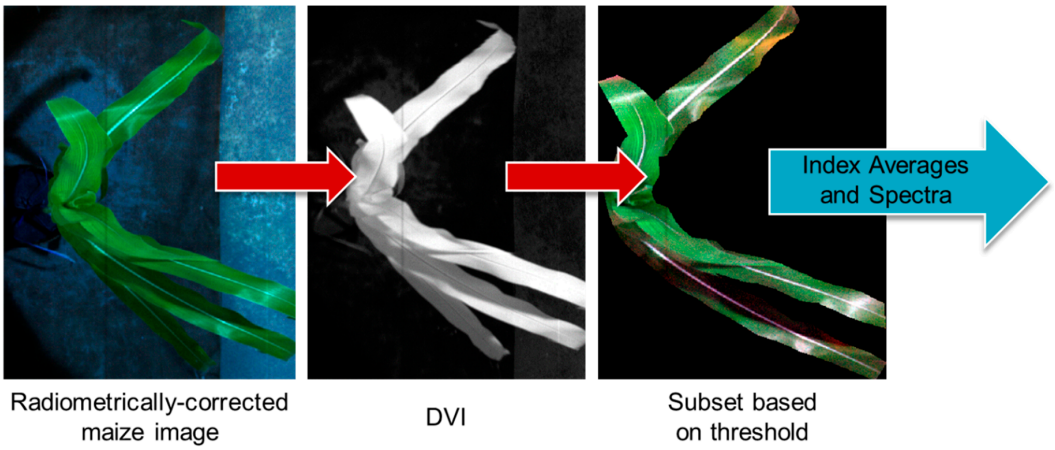

Figure 2. Image processing workflow. The Difference Vegetation Index was used to create a mask on radiometrically-corrected images with a threshold of values. Once masked, reflectance indices are only calculated and averaged on parts of images containing vegetation. Reflectance Index averages and reflectance spectra were then output for statistical analyses. Indices and spectra were averaged pixel-by-pixel for each image.

2.3. Statistics

Reflectance Index values were statistically analyzed in RStudio (RStudio, Inc, Boston, MA) with a one-way analysis of variance (ANOVA) with a least significant difference (LSD) post hoc multiple comparisons test ($\alpha = 0.05$) to obtain *p*-values across plant types and groups. Average reflectance Index values were also used in Principal component analyses (PCA; PC-ORD software ver 5.10, MjM Software, Gleneden Beach, OR) to visualize separation between groups. Spectra of each group were compared via t-tests by using the average reflectance at each waveband (SPSS; $\alpha = 0.05$) to delineate significantly different wavelengths.

Table 1. Indices evaluated for drought and control groups. One-way ANOVA ($\alpha = 0.05$) *p*-values are reported for significant differences between groups. Bold *p*-values indicate significance.

Control – Drought				Plant Type		
Index	**Acronym**	**Relates to**	**References**	**AM**	**AMX**	**S**
Green Difference Vegetation Index	GDVI	Biomass	[21]	**0.0157**	**0.0001**	**0.0057**
Leaf Area Index	LAI		[22]	0.0711	**0.0415**	0.8420
Normalized Difference Vegetation Index	NDVI		[23]	0.6455	0.8991	0.9290
Green Ratio Vegetation Index	GRVI	Photosynthesis	[21]	0.9968	**0.0176**	**0.0027**
Modified Red Edge Simple Ratio	MRESR		[24]	0.5161	0.1252	0.8249
Photochemical Reflectance Index	PRI		[25]	0.7440	**0.0340**	**0.0070**
Anthocyanin Reflectance Index 1	ARI1	Pigments	[26]	0.1553	**0.0008**	**0.0002**
Anthocyanin Reflectance Index 2	ARI2		[26]	0.9573	**0.0056**	**<0.0001**
Carotenoid Reflectance Index 1	CRI1		[27]	0.9999	**0.0002**	0.9985
Carotenoid Reflectance Index 2	CRI2		[27]	0.9219	**0.0002**	0.7921
Green Normalized Difference Vegetation Index	GNDVI		[28]	0.9999	0.1213	**0.0396**
Modified Chlorophyll Absorption Ratio Index	MCARI		[29]	0.0994	**0.0080**	0.5899
Structure-Insensitive Pigment Index	SIPI		[30]	0.9933	0.8080	0.9129
Vogelmann Red Edge Index 1	VREI1		[31]	0.1114	0.1947	0.4924
Vogelmann Red Edge Index 2	VREI2		[31]	**0.0039**	0.0602	0.9844
Plant Senescence Reflectance Index	PSRI	Stress	[32]	0.4803	0.9719	0.5158
Red Edge Position Index	REPI		[33]	0.3607	0.6276	0.7286
Water Band Index	WBI	Water Content	[34]	0.9125	0.8755	**<0.0001**

3. Results

The custom imaging system provided hyperspectral reflectance data that differentiated among RDX exposure and control and drought groups. Data indicated that maize hybrids and sorghum had significant responses as water stress and explosives treatments were discernable using HSI. One-way ANOVA ($\alpha = 0.05$) revealed differences between each group by the end of the experiment. *p*-Values between control and drought groups of AM, AMX, and S indicated that two, nine, and seven indices were affected by water stress, respectively (Table 1). The number of indices significantly altered by RDX in soil, relative to controls, for AM, AMX, and S was 17, 15, and 15, respectively (Table 2). Between drought and RDX treatments, 17 indices differed for both the AM the AMX hybrid, and 16 for S (Table 3). The green ratio vegetation Index (GRVI; Figure 3a) of all plant types was reduced due to the presence of explosives compared to control plants and drought plants. Drought plants of AMX and S showed slight increases in GRVI, relative to controls (*p*-values = 0.0176 and 0.0027, respectively).

Table 2. Indices evaluated for control and RDX groups. One-way ANOVA ($\alpha = 0.05$) *p*-values are reported for significant differences between groups. Bold *p*-values indicate significance.

Control – RDX				Plant Type		
Index	**Acronym**	**Relates to**	**References**	**AM**	**AMX**	**S**
Green Difference Vegetation Index	GDVI	Biomass	[21]	**0.0002**	**<0.0001**	0.9979
Leaf Area Index	LAI		[22]	**<0.0001**	**<0.0001**	**<0.0001**
Normalized Difference Vegetation Index	NDVI		[23]	**<0.0001**	**<0.0001**	**<0.0001**
Green Ratio Vegetation Index	GRVI	Photosynthesis	[21]	**<0.0001**	**<0.0001**	**0.0048**
Modified Red Edge Simple Ratio	MRESR		[24]	**<0.0001**	**<0.0001**	**<0.0001**
Photochemical Reflectance Index	PRI		[25]	**<0.0001**	**<0.0001**	**<0.0001**
Anthocyanin Reflectance Index 1	ARI1	Pigments	[26]	0.5534	**0.0054**	**<0.0001**
Anthocyanin Reflectance Index 2	ARI2		[26]	**0.0008**	0.6521	**<0.0001**
Carotenoid Reflectance Index 1	CRI1		[27]	**<0.0001**	0.0525	0.0953
Carotenoid Reflectance Index 2	CRI2		[27]	**<0.0001**	0.4028	0.5756
Green Normalized Difference Vegetation Index	GNDVI		[28]	**<0.0001**	**<0.0001**	**0.0040**
Modified Chlorophyll Absorption Ratio Index	MCARI		[29]	**0.0008**	**0.0322**	**<0.0001**
Structure-Insensitive Pigment Index	SIPI		[30]	**0.0017**	**0.0009**	**0.0012**
Vogelmann Red Edge Index 1	VREI1		[31]	**<0.0001**	**<0.0001**	**<0.0001**
Vogelmann Red Edge Index 2	VREI2		[31]	**<0.0001**	**<0.0001**	**<0.0001**
Plant Senescence Reflectance Index	PSRI	Stress	[32]	**<0.0001**	**<0.0001**	**<0.0001**
Red Edge Position Index	REPI		[33]	**<0.0001**	**<0.0001**	**<0.0001**
Water Band Index	WBI	Water Content	[34]	**<0.0001**	**<0.0001**	**<0.0001**

Table 3. Indices evaluated for drought and RDX groups. One-way ANOVA ($\alpha = 0.05$) *p*-values are reported for significant differences between groups. Bold *p*-values indicate significance.

Drought – RDX				Plant Type		
Index	**Acronym**	**Relates to**	**References**	**AM**	**AMX**	**S**
Green Difference Vegetation Index	GDVI	Biomass	[21]	0.1478	**0.0015**	**0.0050**
Leaf Area Index	LAI		[22]	**<0.0001**	**<0.0001**	**<0.0001**
Normalized Difference Vegetation Index	NDVI		[23]	**<0.0001**	**<0.0001**	**<0.0001**
Green Ratio Vegetation Index	GRVI	Photosynthesis	[21]	**<0.0001**	**<0.0001**	**<0.0001**
Modified Red Edge Simple Ratio	MRESR		[24]	**<0.0001**	**<0.0001**	**<0.0001**
Photochemical Reflectance Index	PRI		[25]	**<0.0001**	**<0.0001**	**<0.0001**
Anthocyanin Reflectance Index 1	ARI1	Pigments	[26]	**0.0220**	0.7118	**0.0093**
Anthocyanin Reflectance Index 2	ARI2		[26]	**0.0016**	**0.0406**	**0.0064**
Carotenoid Reflectance Index 1	CRI1		[27]	**<0.0001**	**<0.0001**	0.0740
Carotenoid Reflectance Index 2	CRI2		[27]	**<0.0001**	**<0.0001**	0.2193
Green Normalized Difference Vegetation Index	GNDVI		[28]	**<0.0001**	**<0.0001**	**<0.0001**
Modified Chlorophyll Absorption Ratio Index	MCARI		[29]	**<0.0001**	**<0.0001**	**<0.0001**
Structure-Insensitive Pigment Index	SIPI		[30]	**<0.0001**	**0.0002**	**0.0022**
Vogelmann Red Edge Index 1	VREI1		[31]	**<0.0001**	**<0.0001**	**<0.0001**
Vogelmann Red Edge Index 2	VREI2		[31]	**<0.0001**	**<0.0001**	**<0.0001**
Plant Senescence Reflectance Index	PSRI	Stress	[32]	**<0.0001**	**<0.0001**	**0.0002**
Red Edge Position Index	REPI		[33]	**<0.0001**	**<0.0001**	**<0.0001**
Water Band Index	WBI	Water Content	[34]	0.1478	**0.0015**	**0.0050**

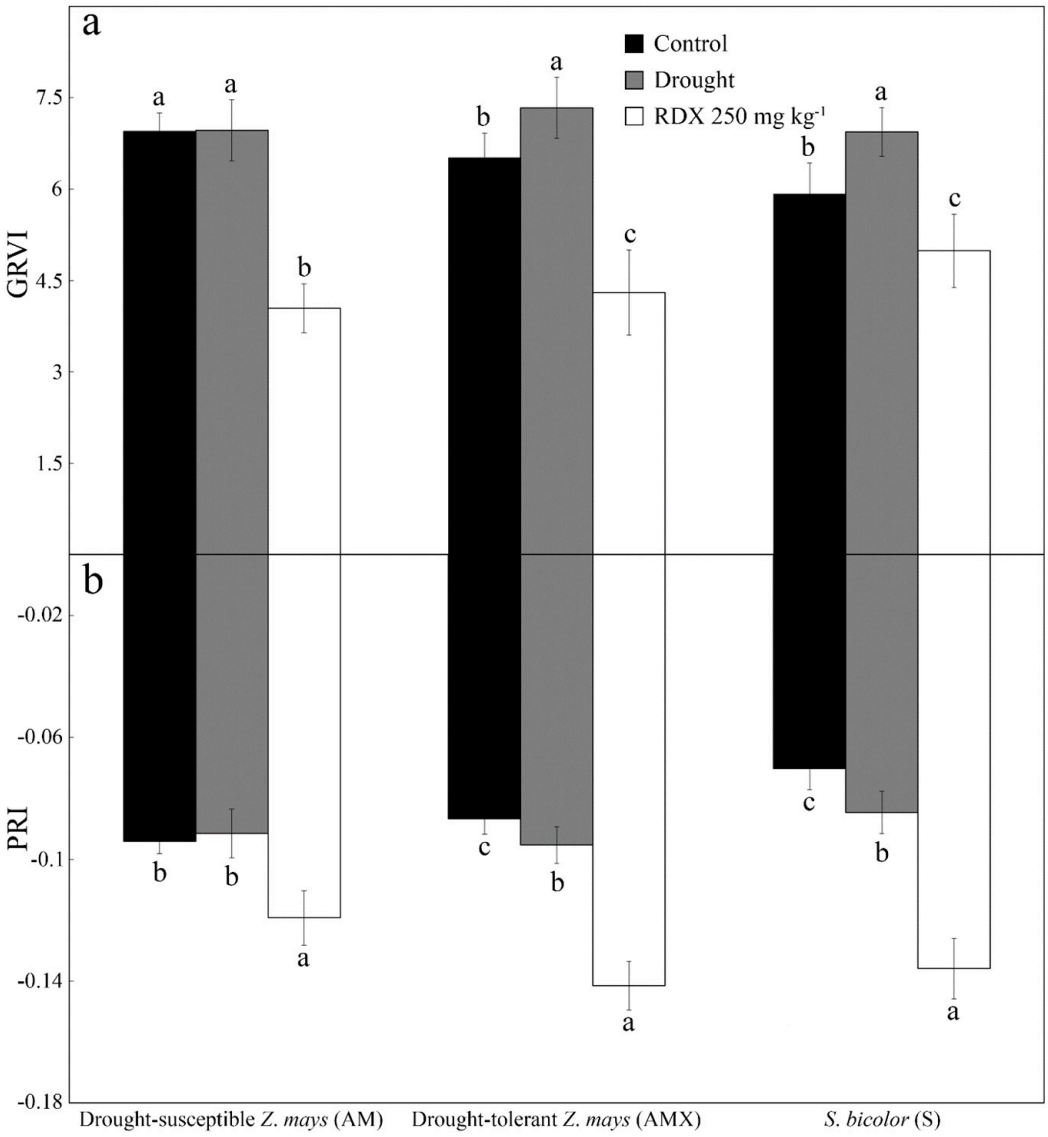

Figure 3. Comparison of reflectance indices for all three plant types and groups: (**a**) Green Ratio Vegetation Index (GRVI) average values. (**b**) Photochemical Reflectance Index (PRI) average values. n = 8 for all groups less *S. bicolor* control (n = 7) and AM *Z. mays* exposed to RDX (n = 7). Error bars represent standard deviations.

The photochemical reflectance Index (PRI) was only slightly increased for drought in AM but was significantly reduced for both drought in AMX (p = 0.0340) and in S (p = 0.0070; Figure 3b). PRI, however, was reduced for all plant types in the RDX treatment (p-values < 0.0001), relative to drought and control plants. The anthocyanin reflectance Index 2 (ARI2) was inconsistent across plant type and groups (Figure 4a). Significant reductions in RDX AM, relative to control and drought plants (p-values = 0.0008 and 0.0016, respectively), differed from AMX and S, where drought and RDX ARI2 values were higher, though at different levels. ARI2 of drought AMX was significantly higher than that of controls (p-value = 0.0056), as it was for RDX (p-value = 0.0406). Drought and RDX ARI2 values of S were also increased when compared to control plants (p-values < 0.0001), with values in the RDX treatment also higher than in the drought treatment (p-value = 0.0064). The RDX treatment caused drastic reductions (p-values < 0.0001) in the modified red edge simple ratio (MRESR) in all plant types, but no differences were found between drought and control plants (Figure 4b). The same response was found for Vogelmann reflectance Index 1 (VRI1; p-values < 0.0001; Figure 4c).

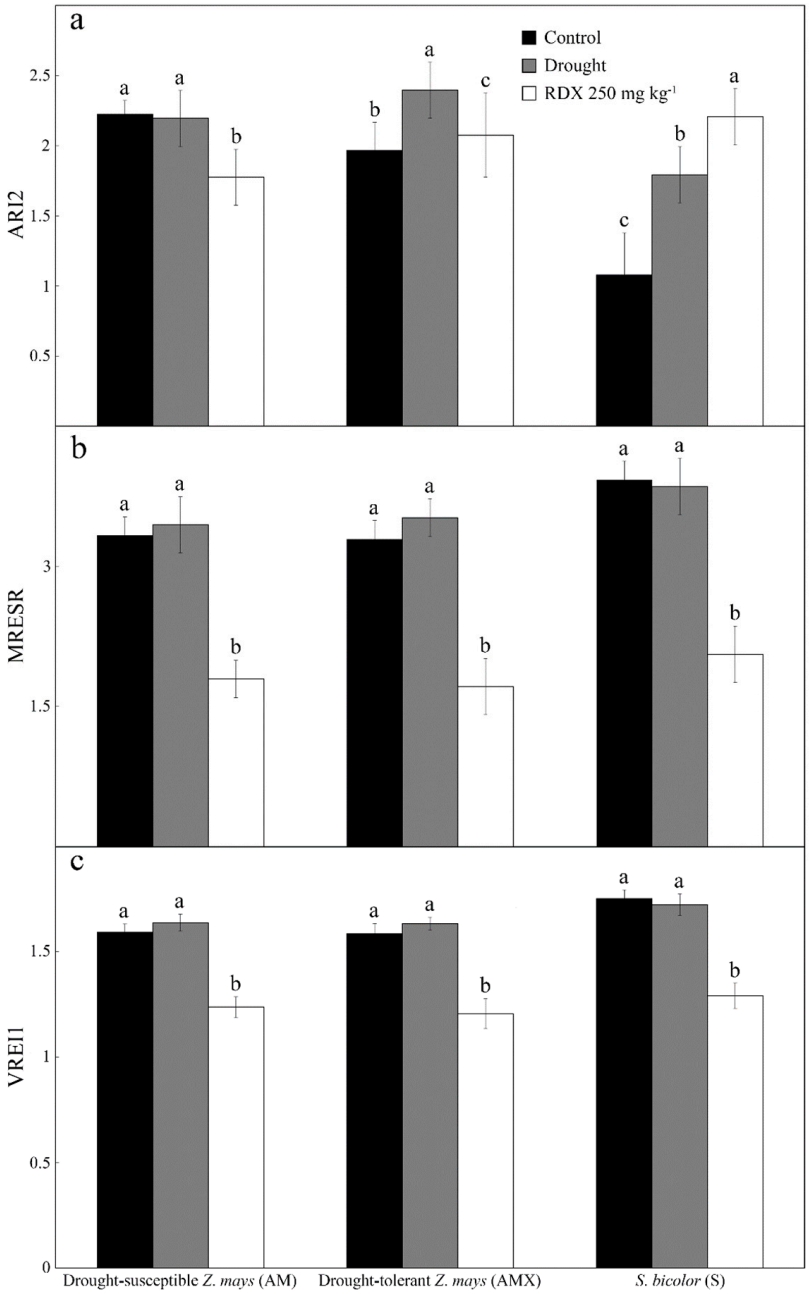

Figure 4. Comparison of reflectance indices for all three plant types and groups: (**a**) Average Anthocyanin Reflectance Index 2 values. (**b**) Modified Red Edge Simple Ratio (MRESR) average values. (**c**) Vogelmann Red Edge Index 1 (VREI1) average values. n = 8 for all groups less *S. bicolor* control (n = 7) and AM *Z. mays* exposed to RDX (n = 7). Error bars represent standard deviations.

To evaluate the dataset for all groups, PCA of reflectance indices was conducted and clearly separated RDX-treated plants from control and drought plants for all plant types (Figure 5). Axis 1 explained 66% of variance with all groups present (Figure 5a). Indices mainly responsible for separation along Axis 1 of RDX-treated plants were related to pigments (MCARI, SIPI, VREI2) and stress (PSRI). Other pigment indices (CRI1, CRI2, VREI), and indices related to biomass (LAI, NDVI) and photosynthesis (GRVI, MRESR, PRI), caused control and drought plants to group to the right.

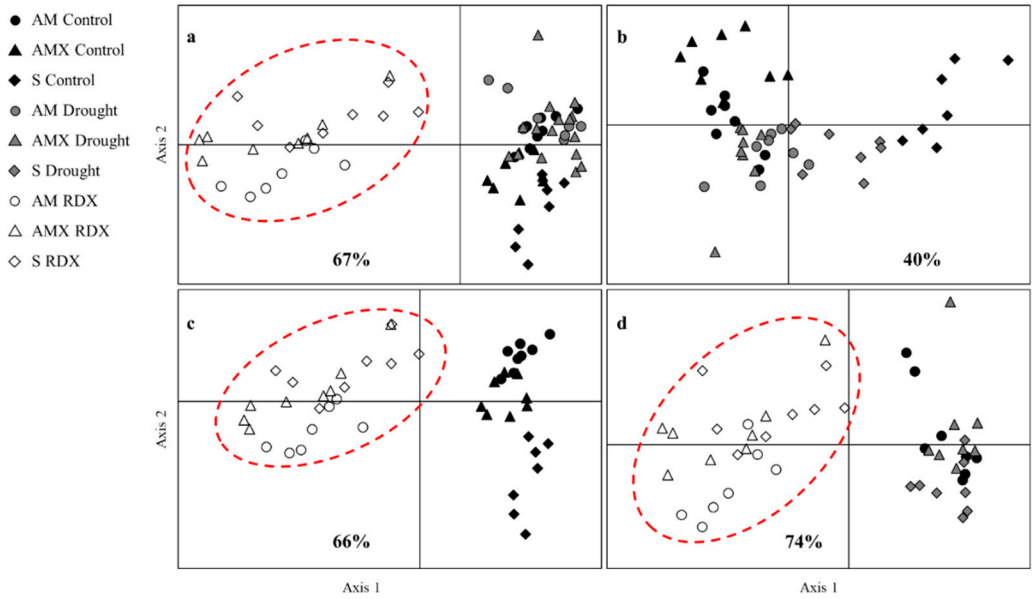

Figure 5. Principle Components Analyses of (**a**) control, drought, and RDX groups; (**b**) control and drought groups; (**c**) control and RDX groups; and (**d**) drought and RDX groups. Each PCA includes all plant types. Ovals indicated separation between groups. Percentages define the variance explained by Axis 1. n = 8 for all groups less *S. bicolor* control (n = 7) and AM *Z. mays* exposed to RDX (n = 7) that had one mortality.

Control and drought plants showed grouping without complete separation (Figure 5b; Axis 1 variance of 39%). Control and RDX plants were completely separated from one another, with Axis 1 accounting for 65% of variance between the two groups (Figure 5c). Drought and RDX groups were also completely separated with 74% of variance explained by Axis 1 (Figure 5d).

Reflectance spectra of each plant was extracted from HSI and averaged by group. Average reflectance spectra of AM in drought revealed significant reductions in reflectance in visible (VIS) and near-infrared (NIR) wavelengths relative to control ($\alpha < 0.05$; Figure 6a). NIR reflectance of AM RDX plants was also significantly reduced relative to controls, though increased in the VIS portion ($\alpha < 0.05$; Figure 6a). Reflectance of AM RDX plants was also higher in VIS wavelengths while similar in the NIR portions, relative to drought plants ($\alpha < 0.05$; Figure 6a). Similar trends were seen in AMX plants with more significantly different wavelengths between drought plants and controls, and less significant wavelengths between RDX plants and controls (Figure 6b). Spectra of S drought plants remained similar to controls from 398–816 nm, then reflectance of drought plants decreased relative to control plants from 817–1000 nm (Figure 6c). S treated with RDX reflected more light from 502–740 nm and along the red edge where it was significantly higher from control and drought plants (Figure 6c). NIR reflectance of RDX plants followed the same trend as drought plants.

Reflectance first derivative averages were calculated from average spectra for each group and plant type. Derivatives of AM plants were similar across groups but showed most variations near 520 nm, 658 nm, and between the red edge to 763 nm (Figure 7a). Drought and RDX first derivatives tracked along control first derivatives in the NIR (Figure 7a). Though the patterns are similar, first derivatives of AMX plants between 476 and 671 nm have gaps between each group. Between 696 and 727 nm, each group's derivative peaked at different wavelengths or values (Figure 7b). AMX RDX plants showed a relatively low derivative value at 696 nm and a more gradual decrease from 696–751 nm (Figure 7b). Smaller variations are present in the remaining NIR wavelengths. Minor differences were present in S first derivatives in VIS wavelengths (Figure 7c). S RDX derivatives deviated the most from control and drought derivatives in the 674–760 range. Overall, control and drought S derivatives were similar to one another.

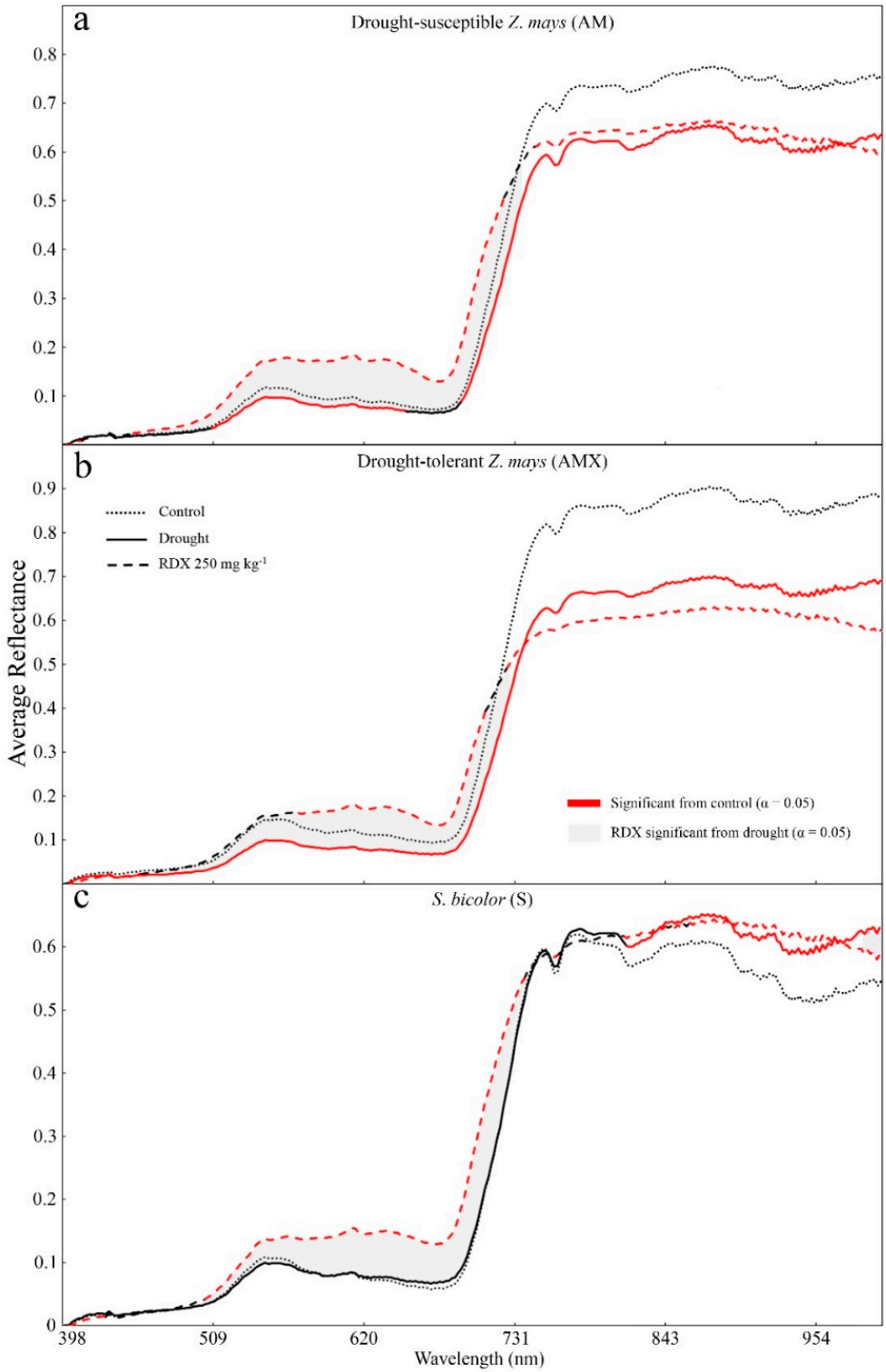

Figure 6. Average reflectance spectra of control, drought, and RDX groups for (**a**) drought-susceptible (AM) *Z. mays*, (**b**) drought-tolerant (AMX) *Z. mays*, and (**c**) *S. bicolor* (S). Line portions in red signify statistical difference from controls ($\alpha = 0.05$). Shaded regions indicate statistical significance between drought and RDX groups ($\alpha = 0.05$). n = 8 for all groups less *S. bicolor* control (n = 7) and AM *Z. mays* exposed to RDX (n = 7).

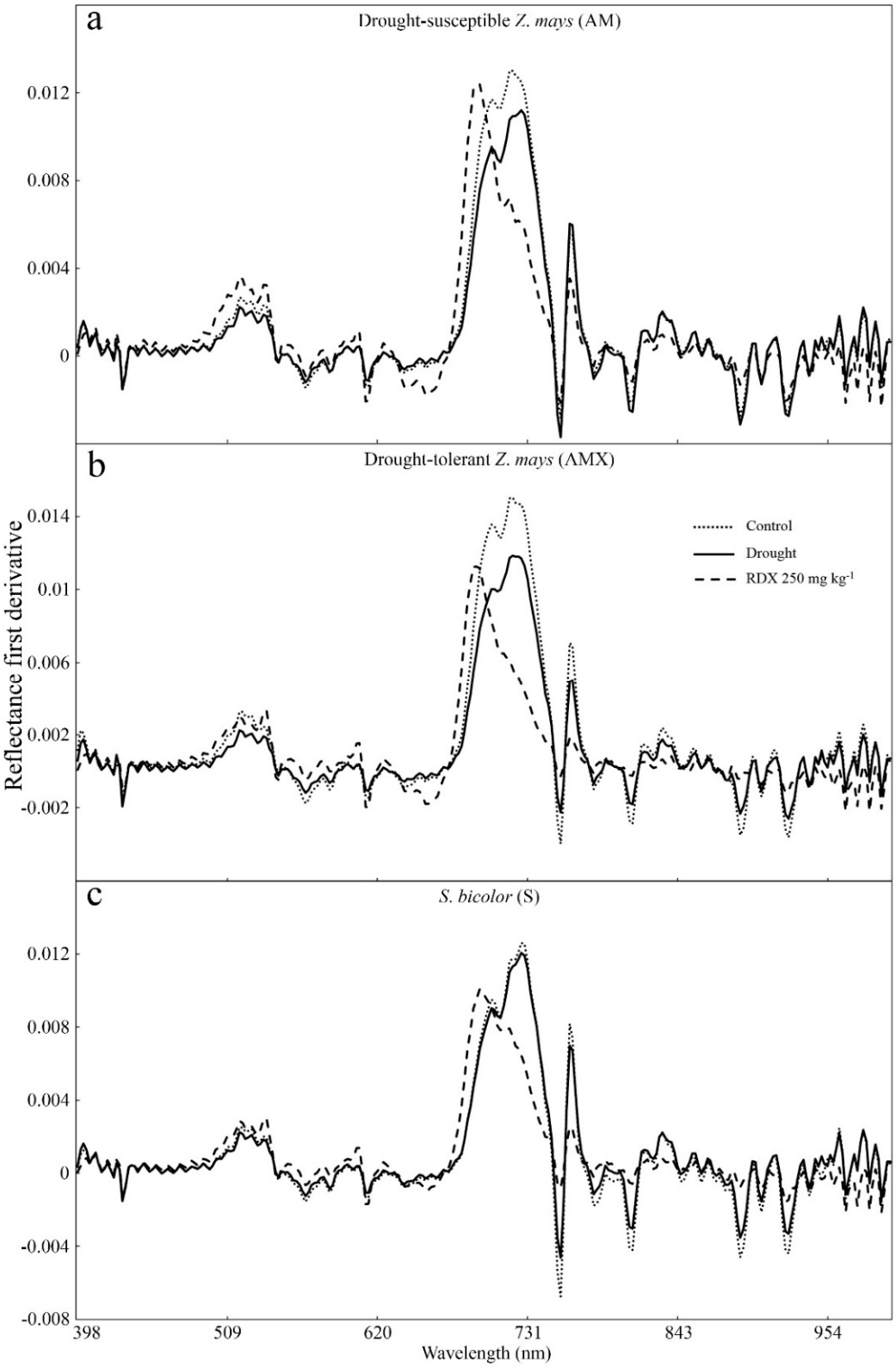

Figure 7. First derivatives of control, drought, and RDX drought-susceptible *Z. mays* (AM) groups calculated and averaged from individual plant spectra. n = 8 for all groups less *S. bicolor* control (n = 7) and AM *Z. mays* exposed to RDX (n = 7).

4. Discussion

RDX is known to be phytotoxic to plants in morphological and physiological ways, though effects are concentration-, and species-dependent [13,17]. Drought also negatively affects plant performance depending on severity. In this study, the effects of drought conditions and exposure to RDX in soil were hypothesized to be discernable from controls but not each other. However, HSI did differentiate between drought and anthropogenic stress from RDX. To ensure plants exposed to RDX would be able to germinate, those seeds were started in clean soil and then transplanted to contaminated soil as explosives are known to inhibit germination of some species [35]. Seeds of other groups were started in clean soil. While only the RDX group potentially underwent stress from transplantation, plants were given a week to recover before the experiment began. One-way ANOVA results of reflectance indices clearly show changes between control and drought group as well as between drought and RDX groups. Drought AM had the lowest number of indices that differed from the control, with only GDVI and VREI2 showing significant deviations. Drought AMX and S were more different from controls based on *p*-values of the one-way ANOVA. Almost all indices were significantly different for control-RDX and drought-RDX comparisons for all plant types indicating plant physiological and morphological responses from RDX exposure that weren't detected under drought conditions (Tables 2 and 3). Only one Index (GDVI) correctly discerned drought plants from controls for all three plant types. Contrarily, 14 reflectance indices were able to distinguish RDX-exposed plants from control and drought plants.

Differences are further evident based on PCAs with clear separation between and clustering of plants by group (Figure 5). Increased variance in PCA results is attributed to reflectance Index values from RDX exposure (Figure 5a,c,d). When considering all groups, indices such as MCARI, PSRI, SIPI, and VREI2 were most responsible for RDX plants to separate along Axis 1. All other indices, less ARI1 and ARI2, strongly accounted for control and drought groups that congregated to the right. The same patterns are also evident when comparing between only two of three groups, with variable percentages of variance explained by Axis 1 (Figure 5b–d). Comparing average Index values (Figures 3 and 4) with PCA results (Figure 5) provides insight into why such variance is present: inconsistencies across plant types in ARI2 (Figure 4a) tied with drastic reductions in other Index values caused such separations in PCA results to occur.

Reflectance spectra for AM and AMX plants showed similar patterns between groups. Control and drought groups for both maize hybrids showed less reflectance in the 500–700 nm (VIS) range compared to that of RDX. This range represents chlorophyll *a* and *b*, carotenoids, and accessory pigments and is used as a non-destructive method to derive pigment concentrations [36]. RDX has been shown to cause reductions in chlorophyll concentrations [13,14] which can be interpreted as increases in reflectance in VIS wavelengths. The red edge, wavelengths from ~700–750 nm, can be indicative of stress by exhibiting a "blue shift", or increased reflectance along the red edge range of wavelengths [37,38]. A red edge that is shifted towards NIR wavelengths is suggestive of higher chlorophyll concentrations [39,40], which AMX expressed. Beyond the red edge into the NIR, are wavelengths that are correlated with plant biomass [41]. High internal scattering of longer wavelengths within leaves caused by cellulose, lignin, and other physical structures intensifies the signal captured compared to reflectance of VIS wavelengths [42]. Drought conditions can hinder photosynthesis and thereby decrease biomass production, but RDX uptake has been reported to not affect biomass, by direct measurement or spectra, at concentrations lower than 500 mg kg^{-1} [16,43] despite reducing rates of photosynthesis [14,16]. However, in this study less intense reflectance in NIR wavelengths was measured (Figure 6a,b) for AM and AMX indicating reduced biomass, accompanied with reductions in the Index correlated to photosynthesis, PRI (Figure 3b). Average reflectance of S showed increased NIR reflectance (Figure 6c) indicating it may be more resistant to drought and anthropogenic stressors negatively affecting biomass, despite reductions in remotely sensed rates of photosynthesis in PRI (Figure 3b).

Vegetation reflectance Index results after four weeks of RDX exposure were mostly indicative of stress dissimilar to drought responses demonstrating that remote sensing of vegetation is promising as a

proxy subsurface forensic tool. Unfortunately, currently existing indices calculated from this experiment are not wholly indicative of stress induced from explosives. Indices related to photosynthesis (GRVI, PRI; Figure 3a,b) were both reduced significantly due to presence of RDX, yet stress indices based on pigment content were not conclusive (ARI2; Figure 4a), as well as others (Tables 2 and 3). What is needed is an explosives-specific Index (ESI), or a toolbox of explosives-specific indices that work well when comparing multiple vegetation and explosives types to respective unexposed plants. One way to begin exploring for wavelengths suitable for Index development is through the calculation of reflectance first derivatives (Figure 7).

First derivatives calculated from average reflectance spectra are effective at highlighting where specific wavelengths and portions of spectra differ based on changes in slope. Drought and control group first derivatives tracked relatively consistently for all tested plant types (Figure 7). While the forms are similar for AM and AMX control and drought average derivatives, differences in intensity were evident in green wavelengths and red edge wavelengths (Figure 7a,b). Control and drought S first derivatives were almost identical throughout, less a few specific wavelengths (Figure 7c). Thus, these differences can be beneficial to Index development to expand the set of tools from which to draw useful water stress indices.

Many of the wavelengths where derivatives indicated changes in reflectance responses to water stress were close to those that were affected by RDX exposure, however in different ways. For example, the values of local minima in NIR wavelengths (750–1000 nm) for AMX and S differ between drought and control plants while RDX plants do not seem to dip at all and track in a more level manner for NIR wavelengths (Figure 7b,c). Key areas for exploration and development of an ESI, or an ESI toolbox, lie in the green wavelengths, red edge, and some NIR wavelengths. When considering wavelengths for Index development, limiting both false positives and negatives is imperative for the successful application of this technique of remotely detecting explosives via plant uptake to field scenarios including, but not limited to, remote detection of indiscriminately-laid, remnant landmines from previous wars and conflicts. Resulting ESIs could also be applied to explosives production and testing sites, as there is a great risk of contaminating soil and groundwater whenever explosives are produced, transported, and tested [8,44].

Explosive compounds can be phytotoxic, with symptoms including leaf curling, chlorotic and necrotic lesions on leaves, and leaf drop [14,45,46]. Plant functioning is also affected and may be assessed through chlorophyll concentrations, fluorescence, and photosynthesis measurements. These effects on plant physiology and morphology can be detected and quantified via hyperspectral imaging remotely over large areas, which has been used for decades to detect plant stress before it is visible to the naked eye in efforts to limit reductions in agricultural crop yields, as well as to detect various sources of contamination [47,48]. Using reflectance indices as a metric to estimate parameters such as chlorophyll content, photosynthesis, and biomass may allow for the high-throughput determination of not only plant stress, but the cause of stress, a necessary distinction when sensing for dangerous explosive compounds. While current indices will be of use for traditional stress responses that may result from explosives exposure, the development of an explosives-specific Index or set of indices will aide in reducing false positives to more accurately pinpoint plants that have absorbed energetics. Enhancing currently existing remote sensing technologies may be useful in detecting chemical exposure in plants in the search for remnant landmines, other types of UXO, and contamination from a variety of sources. Further research is underway to explore key wavelengths from reflectance derivatives, as well as continuing to expand the types of species and explosives tested to better understand the relationship between plants and xenobiotics for developing remote sensing techniques.

5. Conclusions

The results presented validate methods to delineate subsurface explosives over large areas at a canopy scale using the remote sensing of vegetation with aerial-based hyperspectral systems. Current detection methods for fugitive chemicals are all located within the minefields themselves and include

people using electronic mine detectors or leading animals trained to smell explosives on leashes [49,50]. These methods are time-consuming, expensive, and require people to work in close proximity to mines. Plants are also considered a hindrance to conventional mine detection and removal methods. Using HSI for contaminated areas that are vegetated could be highly informative and applicable over large areas in a relatively short amount of time. Within these datasets, spectral characteristics may indicate the location of contamination based on vegetation's ability to take up explosives and consequent impact of these explosives on plant form and function. The methods developed herein can be directly applied to assess potential landmine locations as well as translated to assess a wide variety of environmental contaminants that have plant stress responses. Such remote sensing methods can not only speed up landmine detection and remediation, but also make it safer by removing people from minefields during the detection process. The development and implementation of ESIs from HSI may be beneficial towards that goal.

Author Contributions: The conceptualization and methodology of this research was devised by J.G.B. and P.V.M. Investigation, data curation, and formal analysis was performed by P.V.M. with supervision from J.G.B. and V.S. Funding acquisition and project administration was from J.G.B. Resources were acquired from F.B.F. and J.G.B. Software was handled by P.V.M. with help from V.S. Validation was performed by J.G.B., F.B.F., and V.S. Visualization was performed by P.V.M. Writing—original draft was prepared by Paul Manley and J.G.B. Writing—review & editing was performed by all authors.

Funding: This research was conducted through Missouri EPSCoR, which is funded by the National Science Foundation under Award #IIA-1355406 and #IIA-1430427.

Acknowledgments: The authors would like to thank the editor and reviewers for their diligent work in maintaining the quality of this journal.

Conflicts of Interest: The authors declare no conflict of interest. The funders had no role in the design of the study; in the collection, analyses, or interpretation of data; in the writing of the manuscript, or in the decision to publish the results.

References

1. U.S. Environmental Protection Agency. Available online: https://cfpub.epa.gov/ncea/iris/iris_documents/documents/toxreviews/0313tr.pdf (accessed on 23 March 2019).
2. Walsh, N.E.; Walsh, W.S. Rehabilitation of landmine victims—The ultimate challenge. *Bull. World Health Organ.* **2003**, *81*, 665–670. [PubMed]
3. Strada, G. The horror of land mines. *Sci. Am.* **1996**, *274*, 40–45. [CrossRef]
4. Rylott, E.L.; Bruce, N.C. Plants disarm soil: Engineering plants for the phytoremediation of explosives. *Trends Biotechnol.* **2009**, *27*, 73–81. [CrossRef] [PubMed]
5. Rylott, E.L.; Budarina, M.V.; Barker, A.; Lorenz, A.; Strand, S.E.; Bruce, N.C. Engineering plants for the phytoremediation of RDX in the presence of the co-contaminating explosive TNT. *New Phytol.* **2011**, *192*, 405–413. [CrossRef] [PubMed]
6. U.S. Environmental Protection Agency. Available online: https://www.epa.gov/sites/production/files/documents/ifuxoctthandbook.pdf (accessed on 7 February 2019).
7. MacDonald, J.A.; Small, M.J.; Granger Morgan, M. Quantifying the risks of unexploded ordnance at closed military bases. *Environ. Sci. Technol.* **2009**, *43*, 259–265. [CrossRef] [PubMed]
8. Taylor, S.; Bigl, S.; Packer, B. Condition of *in situ* unexploded ordnance. *Sci. Total Environ.* **2015**, *505*, 762–769. [CrossRef] [PubMed]
9. Limmer, M.; Burken, J. Phytovolatilization of organic contaminants. *Environ. Sci. Technol.* **2016**, *50*, 6632–6643. [CrossRef] [PubMed]
10. Burken, J.G.; Vroblesky, D.A.; Balouet, J.C. Phytoforensics, dendrochemistry, and phytoscreening: New green tools for delineating contaminants from past and present. *Environ. Sci. Technol.* **2011**, *45*, 6218–6226. [CrossRef] [PubMed]
11. Ghosh, M.; Singh, S.P. A review on phytoremediation of heavy metals and utilization of it's by products. *Asian J. Energy Environ.* **2005**, *6*, 214–231.
12. Singh, S.N.; Mishra, S. Phytoremediation of TNT and RDX. In *Biological Remediation of Explosive Residues*; Springer: Cham, Switzerland; New York, NY, USA, 2014; pp. 371–392. [CrossRef]

13. Vila, M.; Lorber-Pascal, S.; Laurent, F. Fate of RDX and TNT in agronomic plants. *Environ. Pollut.* **2007**, *148*, 148–154. [CrossRef] [PubMed]
14. Zinnert, J.C. Plants as phytosensors: Physiological responses of a woody plant in response to RDX exposure and potential for remote detection. *Int. J. Plant Sci.* **2012**, *173*, 1005–1014. [CrossRef]
15. Barton, C.V.M. Advances in remote sensing of plant stress. *Plant Soil* **2012**, *354*, 41–44. [CrossRef]
16. Zinnert, J.C.; Via, S.M.; Young, D.R. Distinguishing natural from anthropogenic stress in plants: Physiology, fluorescence and hyperspectral reflectance. *Plant Soil* **2013**, *366*, 133–141. [CrossRef]
17. Chen, D.; Liu, Z.L.; Banwart, W. Concentration-dependent RDX uptake and remediation by crop plants. *Environ. Sci. Pollut. Res.* **2011**, *18*, 908–917. [CrossRef] [PubMed]
18. Naumann, J.C.; Anderson, J.E.; Young, D.R. Remote detection of plant physiological responses to TNT soil contamination. *Plant Soil* **2010**, *329*, 239–248. [CrossRef]
19. Horler, D.N.H.; Barber, J.; Darch, J.P.; Ferns, D.C.; Barringer, A.R. Approaches to detention of geochemical stress in vegetation. *Adv. Space Res.* **1983**, *3*, 175–179. [CrossRef]
20. Naumann, J.C.; Anderson, J.E.; Young, D.R. Linking physiological responses, chlorophyll fluorescence and hyperspectral imagery to detect salinity stress using the physiological reflectance Index in the coastal shrub, *Myrica cerifera*. *Remote Sens. Environ.* **2008**, *112*, 3865–3875. [CrossRef]
21. Sripada, R.P.; Heiniger, R.W.; White, J.G.; Meijer, A.D. Aerial color infrared photography for determining early in-season nitrogen requirements in corn. *Agron. J.* **2006**, *98*, 968–977. [CrossRef]
22. Boegh, E.; Soegaard, H.; Broge, N.; Hasager, C.; Jensen, N.; Schelde, K.; Thomsen, A. Airborne multi-spectral data for quantifying leaf area Index, nitrogen concentration and photosynthetic efficiency in agriculture. *Remote Sens. Environ.* **2002**, *81*, 179–193. [CrossRef]
23. Rouse, J.; Haas, R.; Schell, J.; Deering, D. Monitoring vegetation systems in the Great Plains with ERTS. In Proceedings of the Third ERTS Symposium, NASA, Washington, DC, USA, 10–14 December 1973; pp. 309–317.
24. Sims, D.A.; Gamon, J.A. Relationships between leaf pigment content and spectral reflectance across a wide range of species, leaf structures and developmental stages. *Remote Sens. Environ.* **2002**, *81*, 337–354. [CrossRef]
25. Gamon, J.A.; Peñuelas, J.; Field, C.B. A narrow-waveband spectral Index that tracks diurnal changes in photosynthetic efficiency. *Remote Sens. Environ.* **1992**, *41*, 35–44. [CrossRef]
26. Gitelson, A.; Merzlyak, M.N.; Chivkunova, O.B. Optical properties and nondestructive estimation of anthocyanin content in plant leaves. *Photochem. Photobiol.* **2001**, *71*, 38–45. [CrossRef]
27. Gitelson, A.A.; Zur, Y.; Chivkunova, O.B.; Merzlyak, M.N. Assessing carotenoid content in plant leaves with reflectance spectroscopy. *Photochem. Photobiol.* **2002**, *75*, 272–281. [CrossRef]
28. Gitelson, A.A.; Merzlyak, M.N. Remote estimation of chlorophyll content in higher plant leaves. *Int. J. Remote Sens.* **1997**, *18*, 2691–2697. [CrossRef]
29. Daughtry, C.S.T.; Walthall, C.L.; Kim, M.S.; Brown de Colstoun, E.; McMurtry, J.E., III. Estimating corn leaf chlorophyll concentration from leaf and canopy reflectance. *Remote Sens. Environ.* **2000**, *74*, 229–239. [CrossRef]
30. Peñuelas, J.; Baret, F.; Filella, I. Semi-empirical indices to assess carotenoids/chlorophyll-a ratio from leaf spectral reflectance. *Photosynthetica* **1995**, *31*, 221–230.
31. Vogelmann, J.E.; Rock, B.N.; Moss, D.M. Red edge spectral measurements from sugar maple leaves. *Int. J. Remote Sens.* **1993**, *14*, 1887–1905. [CrossRef]
32. Merzlyak, M.N.; Gitelson, A.A.; Chivkunova, O.B.; Rakitin, V.Y. Non-destructive optical detection of pigment changes during leaf senescence and fruit ripening. *Physiol. Plant.* **1999**, *106*, 135–141. [CrossRef]
33. Curran, P.; Windham, W.; Gholz, H. Exploring the relationship between reflectance red edge and chlorophyll concentration in slash pine leaves. *Tree Physiol.* **1995**, *15*, 203–206. [CrossRef]
34. Peñuelas, J.; Filella, I.; Biel, C.; Serrano, L.; Savé, R. The reflectance at the 950-970 nm region as an indicator of plant water status. *Int. J. Remote Sens.* **1993**, *14*, 1887–1905. [CrossRef]
35. Via, S.M.; Zinnert, J.C.; Young, D.R. Differential effects of two explosive compounds on seed germination and seedling morphology of a woody shrub, *Morella cerifera*. *Ecotoxicology* **2015**, *24*, 194–201. [CrossRef]
36. Hallik, L.; Kazantsev, T.; Kuusk, A.; Galmes, J.; Tomas, M.; Niinemets, U. Generality of relationships between leaf pigment contents and spectral vegetation indices in Mallorca (Spain). *Reg. Environ. Chang.* **2017**, *17*, 2097–2109. [CrossRef]

37. Gates, D.M.; Keegan, H.J.; Schleter, J.C.; Weidner, V.R. Spectral properties of plants. *Appl. Opt.* **1965**, *4*, 11–20. [CrossRef]
38. Zagajewski, B.; Tommervik, H.; Bjerke, J.W.; Raczko, E.; Bochenek, Z.; Klos, A.; Jarocinska, A.; Lavender, S.; Ziolgkowski, D. Intraspecific differences in spectral reflectance curves as indicators of reduced vitality in high-arctic plants. *Remote Sens.* **2017**, *9*, 1289. [CrossRef]
39. Chappelle, E.W.; Kim, M.S.; McMurtrey, J.E. The red edge shift: An explanation of its relationship to stress and the concentration of chlorophyll a. In Proceedings of the IGARSS'91 Remote Sensing: Global Monitoring for Earth Management, Espoo, Finland, 3–6 June 1991. [CrossRef]
40. Sanches, I.D.; Souza Filho, C.R.; Magalhaes, L.A.; Quiterio, G.C.M.; Alves, M.N.; Oliveira, W.J. Assessing the impact of hydrocarbon leakages on vegetation using reflectance spectroscopy. *ISPRS J. Photogramm. Remote Sens.* **2013**, *78*, 85–101. [CrossRef]
41. Colwell, J.E. Vegetation canopy reflectance. *Remote Sens. Environ.* **1974**, *3*, 175–183. [CrossRef]
42. Curran, P.J. Remote sensing of foliar chemistry. *Remote Sens. Environ.* **1989**, *30*, 271–278. [CrossRef]
43. Best, E.P.H.; Smith, T.; Hagen, F.L. *Candidate Herbaceous Plants for Phytoremediation of Energetics on Ranges*; Technical Report ERDC TR-07-11; U.S. Army Engineer Research and Development Center: Vicksburg, MS, USA, 2007.
44. Taylor, S.; Lever, J.H.; Bostick, B.; Walsh, M.R.; Walsh, M.E.; Packer, B. *Underground UXO: Are They a Significant Source of Explosives in Soil Compared to Low- and High-Order Detonation*; ERDC/CRREL Technical Report TR-04-23; Cold Regions Research and Engineering Laboratory: Hanover, NH, USA, 2004.
45. Rylott, E.L.; Jackson, R.G.; Edwards, J.; Womack, G.L.; Seth-Smith, H.M.B.; Rathbone, D.A.; Strand, S.E.; Bruce, N.C. An explosive-degrading cytochrome P450 activity and its targeted application for the phytoremediation of RDX. *Nat. Biotechnol.* **2006**, *24*, 216–219. [CrossRef] [PubMed]
46. Panz, K.; Miksch, K.; Sojka, T. Synergetic toxic effect of an explosive material mixture in soil. *Bull. Environ. Contam. Toxicol.* **2013**, *91*, 555–559. [CrossRef] [PubMed]
47. Haboudane, D.; Miller, J.R.; Pattev, E.; Zarco-Tejada, P.J.; Stachan, I.B. Hyperspectral vegetation indices and novel algorithms for predicting green LAI of crop canopies: Modeling and validation in the context of precision agriculture. *Remote Sens. Environ.* **2004**, *90*, 337–352. [CrossRef]
48. Slonecker, T.; Fisher, G.B.; Aiello, D.P.; Haack, B. Visible and infrared remote imaging of hazardous waste: A review. *Remote Sens.* **2010**, *2*, 2474–2508. [CrossRef]
49. Leeneer, I.; Pastijn, H. Selecting land mine detection strategies by means of outranking MCDM techniques. *Eur. J. Oper. Res.* **2002**, *139*, 327–338. [CrossRef]
50. Habib, M.K. Controlled biological and biomimetic systems for landmine detection. *Biosens. Bioelectron.* **2007**, *23*, 1–18. [CrossRef] [PubMed]